DOI 10.24425/aee.2021.136994

Safety evaluation for a high signal operator with electric field exposure induced by contact wires

CHANG-QIONG YANG, MAI LU

Lanzhou Jiaotong University
China
e-mail: mai.lu@hotmail.com, (corresponding author), lily_yang05@163.com

(Received: 11.10.2020, revised: 14.01.2021)

Abstract: To evaluate the occupational safety of a high signal operator exposed to the electric field induced by contact wires with a frequency of 50 Hz and a voltage of 27.5 kV, this study established a model of a high signal operator working in the vicinity of single- and double-track railways. The electric field distribution in the operator's body and his head were calculated and analyzed during the operation using the finite element method (FEM). The calculated results were compared with the international standard occupational exposure limits formulated by the International Commission on Non-Ionizing Radiation Protection (ICNIRP) and action levels (ALs), exposure limit values (ELVs) in Directive 2013/35/EU (EU Directive). In the case of a single-track railway exposure, the maximum electric field strength in the worker's body, in the scalp layer, and inside the brain are 227 mV/m, 2.76 kV/m, and 0.14 mV/m, respectively. For a double-track railway exposure, the maximum internal electric field strength of the operator is 310 mV/m, which is 37.85% of the occupational exposure basic restriction limit. The maximum electric field strength in the head layers is 3.42 kV/m, which is 34.2% of the occupational exposure reference level and 34.2% of the low ALs. The maximum electric field strength of the brain is 0.19 mV/m, which is 0.19% of the occupational basic restriction limit and 0.135% of the sensory effects ELVs. Results show that the electric field exposure of the high signal operator to contact wires in single- and double-track railways is lower than the occupational exposure limits provided by the ICNIRP and EU Directive standards and is thus regarded as safe for workers.

Key words: contact wires, electric field, finite element method (FEM), high signal operator, ICNIRP standards, occupational exposure, safety evaluation

1. Introduction

A single-phase power supply mode (50 Hz, 27.5 kV) is mainly used in electrified railways in China. The train pantograph comes into touch with the contact wire to obtain kinetic energy. As the left-hand driving system is implemented in China, the corresponding high or low signal under normal circumstances is set on the left side of the railway line according to operation requirements. Typically, any signal fault is repaired or maintained by signal operators. Hence, the signal operator is exposed to a high voltage power and low frequency electric field environment, where contact wires are located at a short distance from the worker.

In recent years, researchers have conducted in-depth research on the health effects [1] and health risks [2, 3] of extremely low-frequency electromagnetic fields, including 50 Hz power frequency. Paper [3] was the first that studied the effects of extremely low-frequency electromagnetic fields on human health by observing children living near high current distribution lines. The results showed that such exposure increases the probability of leukemia, lymphoma, and nervous system tumors. Study [4] has shown that short-term exposure to a high voltage power and low frequency environment poses a threat to kidneys of rats. In [5], the authors have shown that if there is a safe distance for employees with stents implanted in the body, the interaction of the line on the stent is negligible. Paper [6] assessed the safety of pectus patients with a concave Nuss bar-implant exposed to a plane wave with a frequency of 64 MHz, using the finite-difference time-domain (FDTD) method. The results showed that the concave Nuss bar-implant poses no risk during environmental and occupational RF field exposures.

The research on the electromagnetic field of an electrified railway mainly focuses on the influence between devices [7–9]. However, the health risks of a high voltage electromagnetic environment on occupational exposure to contact wires have rarely been discussed in publications. When signal operators work on high signals, they are much closer to contact wires than the passengers in a carriage. Moreover, they perform their work with no shielding. Therefore, studying the electric field of the surrounding space of high-voltage contact wires is important in the health risk assessment of the high signal operator.

This study uses the FEM-based software COMSOL Multiphysics to calculate the electric field distribution inside the human body, on the head surface, and inside the head of a high signal operator working on single- and double-track railways. In the next step, the calculation results are compared with the current guidelines for limiting time-varying electric fields, magnetic fields, and electromagnetic exposure provided by the International Commission on Non-Ionizing Radiation Protection (ICNIRP) [10], as well as action levels (ALs) and exposure limit values (ELVs) in Directive 2013/35/EU (EU Directive) [11]. This work aims to evaluate the safety of high signal operators exposed to the electric field environment and provide the necessary reference for the development of railway technology in China.

2. Methods and models

Relative locations of a high signal, contact wires, tracks, locomotive, and a pantograph are shown in Fig. 1.

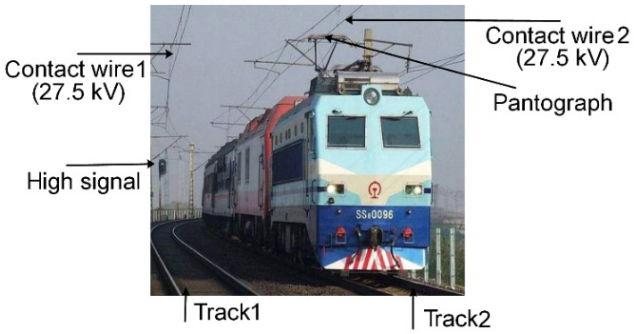

Fig. 1. Relative position of a high signal, pantograph, tracks, and a contact wires [12]

As shown in Fig. 1, a double-track railway has two tracks. In general, a single-track railway has only one track. In the figure, contact wire 1 provides electric energy to the trains running on track 1. Contact wire 2 provides electric energy to the trains running on track 2. The train running on track 2 obtains kinetic energy through the pantograph contacting contact wire 2. The signal operator works on the signal pole when the signal lights need to be repaired or maintained. The electromagnetic field exposure risk during signal maintenance by a signal operator is shown in Fig. 2.

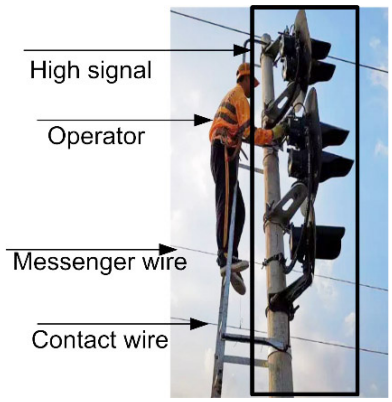

Fig. 2. Operator working on a high signal near the overhead traction lines [13]

2.1. Basic principle of calculating electric field intensity of human body

For electrified railways, the power supply mode adopts an extremely low frequency of 50 Hz, so we are dealing with an electrostatic field. It was assumed that all the modelled materials are considered as isotropic, homogeneous and linear media. Because the electric field distribution within the space around a contact wire is forced by the electric potential applied to the contact wire, the Laplace equation should be employed to solve the described problem [14]:

$$\nabla \cdot (-\sigma \nabla \varphi) = 0, \tag{1}$$

where σ (S/m) and φ (V) mean the electric conductivity of a given medium and the electric potential, respectively.

How to compute the electric field strength $\boldsymbol{E}$ (V/m) and current density $\boldsymbol{J}$ (A/m^2) in operator's body is given by the following equations:

$$\boldsymbol{J} = \sigma \boldsymbol{E}, \tag{2}$$

$$\boldsymbol{E} = \nabla \phi. \tag{3}$$

The boundary conditions along the interfaces between the air and human body tissues or between tissues are considered as:

$$\boldsymbol{N} \cdot (\boldsymbol{J}_1 - \boldsymbol{J}_2) = 0 \tag{4}$$

with the following equivalent form:

$$\boldsymbol{n} \cdot (\sigma_1 \nabla \phi_1 - \sigma_2 \nabla \phi_2) = 0. \tag{5}$$

where $\boldsymbol{n}$ is the normal vector.

2.2. Model in COMSOL Multiphysics

On the one hand, the permittivity and electrical conductivities of human tissues and organs are not the same. Their shapes and volumes are also different. Hence, obtaining satisfactory results with traditional analytical methods is difficult. On the other hand, obtaining the electromagnetic field in human tissues via direct measurements is challenging. It is usually obtained using numerical solution methods [15–18]. The COMSOL Multiphysics is a professional FEM-based software package. It uses the partial differential equations of multiple physical fields and is designed for modeling, simulation, and calculation of approximate solutions. It is widely used in the simulation of electromagnetic effects on a human body under voltage, current, and other electromagnetic fields [19].

In the AC/DC module of COMSOL Multiphysics software, a contact wire, with a length of 10 m, a radius of 6.5 mm, and a distance of 5.7 m above the ground, is established in the Electric Current Interface feature. An air domain with a length of 26 m, a width of 10 m, and a height of 15 m is also considered. The air domain is set as an infinite element domain with a thickness of 10 cm to simulate the edges of a commutation domain. The contact wire is loaded by a voltage of 27.5 kV with a frequency of 50 Hz. The ground is zero potential.

The model of the standing posture of an adult male signal operator with a height of 1.75 m is constructed according to the international adult body proportion [20]. The head model is composed of the scalp, skull, and brain according to the paper [21]. Fig. 3 shows that the center of the lowest light position of the high arrival signal is 5 m from the ground and that the horizontal distance between the center of the column and the center of the line is 2.63 m when the clearance is 2.44 m. Therefore, the human body is localized at 3.75 m above the ground and 2.63 m away from the line. The model construction and its dimensions are shown in Fig. 3. Importantly, the analyzed model with dimensions 26 m $\times$10 m $\times$15 m is solved in a rectangular coordinate system (x, y, z). The computational truncated boundary is electrical insulation.

The relative permittivity and conductivity of human tissues at 50 Hz are calculated according to the database [22]. The brain dielectric parameters consist of average values of brain white

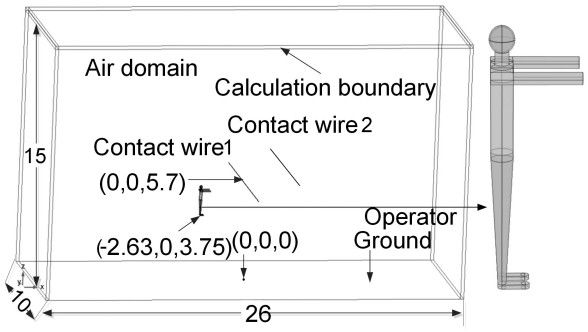

Fig. 3. Simulation model and its dimensions in meters

matter, brain grey matter and cerebrospinal fluid. The average values of muscle, bone cortical and fat are used as the trunk dielectric parameters. The specific values are shown in Table 1. In the model of an operator's body, the corresponding dielectric parameters of human tissues are set according to the data in Table 1.

Table 1. Dielectric parameters of human tissues at a frequency of 50 Hz [22]

Tissues	**Relative permittivity ε_r**	**Electric Conductivity σ (S/m)**
Scalp (skin wet)	5.13×10^4	4.27×10^{-4}
Skull (bone cortical)	8.87×10^3	2.01×10^{-2}
Brain	5.80×10^6	7.09×10^{-1}
Trunk	6.40×10^6	1.51×10^{-1}
Cerebro spinal fluid	1.09×10^2	2.00×10^0
Brain grey matter	1.21×10^7	7.50×10^{-2}
Brain white matter	5.29×10^6	5.33×10^{-2}
Muscle	1.77×10^7	2.33×10^{-1}
Bone cortical	8.87×10^3	2.01×10^{-1}
Fat	1.47×10^6	1.96×10^{-2}

The model is discretized without affecting the accuracy of the calculation results. The whole human body model is divided into tetrahedron elements. For the modelled head, the minimum element size is defined as 1 mm. For the trunk, the minimum element size is set at 10 mm. The discretization results of the human body are shown in Fig. 4.

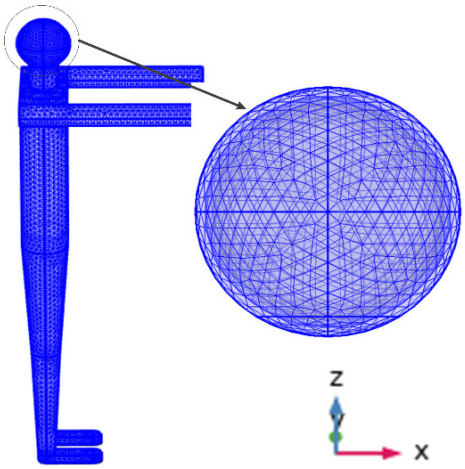

Fig. 4. Three-dimensional finite element mesh of human model

3. Validation of the model

To test the accuracy of the model and estimate the electric field strength around the contact wire using COMSOL Multiphysics software, we used the geometry shown in Fig. 5.

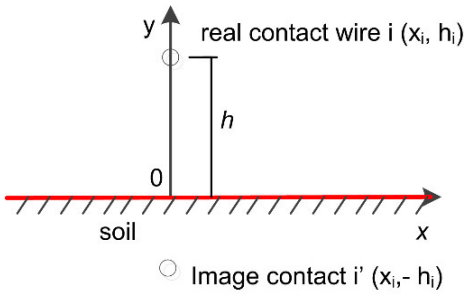

Fig. 5. Geometry used for calculation of electric field

In Fig. 5 the height h from the ground to the contact wire is 5.7 m. The contact wire's radius r is 6.5 mm. The contact wire's voltage is 27.5 kV. The electric field strength on the ground ($x = 0$ m, $y = 0$ m), according to the equations taken from [17,23], is calculated. The calculation process is as follows:

1. The potential coefficient P_i for an i-th wire is calculated by Equation (6) taken from [17]. Then, for wire1: $P_1 = [7.4696 \times (1/(2\pi\varepsilon_0))] = 1.34 \times 10^{-7}$ m/F.

$$P_1 = \frac{1}{2\pi\varepsilon_0} \ln\left(\frac{2h}{r}\right), \tag{6}$$

where: $\varepsilon_0 = 1/(36\pi) \times 10^{-9}$ F/m, r is the conductor radius with a value of 6.5 mm, h is the conductor heigh with a value of 5.7 m.

2. The voltage V_i for an i-th line satisfies with the equation: $Q_i = P_i^{-1}V_i$, In our situation for wire 1, $V_1 = 2.75 \times 10^4$ V. The charge on such a wire is calculated as:

$$Q_1 = [3.6846 \times (2\pi\varepsilon_0)] = 2.047 \times 10^{-10} \text{ C/m}.$$

3. By substituting Q_1 into Equation (7) taken from [17,23], the electric field strength derived from the i-th wire $\boldsymbol{E}_i$ at the ground point is calculated as $\boldsymbol{E}_1 = -1291.8\,\boldsymbol{a}_y$ V/m.

$$E_i = \frac{1}{2\pi\varepsilon_0} Q_1 \left(\begin{array}{l} \left(\dfrac{x - x_i}{(x - x_i)^2 + (y - y_i)^2} - \dfrac{x - x_i}{(x - x_i)^2 + (y + y_i)^2} \right) \boldsymbol{a}_x + \\ + \left(\dfrac{y - y_i}{(x - x_i)^2 + (y - y_i)^2} - \dfrac{y + y_i}{(x - x_i)^2 + (y + y_i)^2} \right) \boldsymbol{a}_y \end{array} \right), \tag{7}$$

where x, y, x_i, and y_i are the coordinates for observation and conductor points. In the analyzed situation, $x = 0$, $y = 0$, $x_i = 0$, and $y_i = 5.7$ m.

In the model shown in Fig. 3, the contact wire is loaded at 50 Hz and 27.5 kV without a high signal operator. The electric field is calculated after dissection and simulated in COMSOL Multiphysics. The comparison between the simulation result and the theoretical calculation value is shown in Table 2.

Table 2. Comparison between simulation and theoretical values of electric field strength

Point	**Simulation value (V/m)**	**Theoretical value (V/m)**	**Simulation value/ Calculation value (%)**
$(x = 0, y = 0, z = 0)$ m	1265.3	1291.8	97.95%

Table 2 shows that the ratio of simulation value to theoretical value is 97.95%, which proves that the model can meet the required engineering calculation accuracy. Moreover, the software can accurately estimate the electric field distribution of the high signal operator in the space around the contact wire.

4. Result analysis

This work analyzes the distribution of electric field strength in the body of a high signal operator, the head surface, and its interior in the cases of single-track railways and double-track railways. The effect of the magnetic field is neglected in this paper.

4.1. Analysis for single-track railway

The simulation model of a single-track railway with contact wire 1 is shown in Fig. 3. The E-field distribution in the body of a high signal operator is shown in Fig. 6.

As shown in Fig. 6(b), the electric field intensity in the high signal operator's body is mainly distributed in the scalp near the contact wire, with the maximum value equal to 227 mV/m. The high signal operator's head is an important part of the central nervous system. To effectively

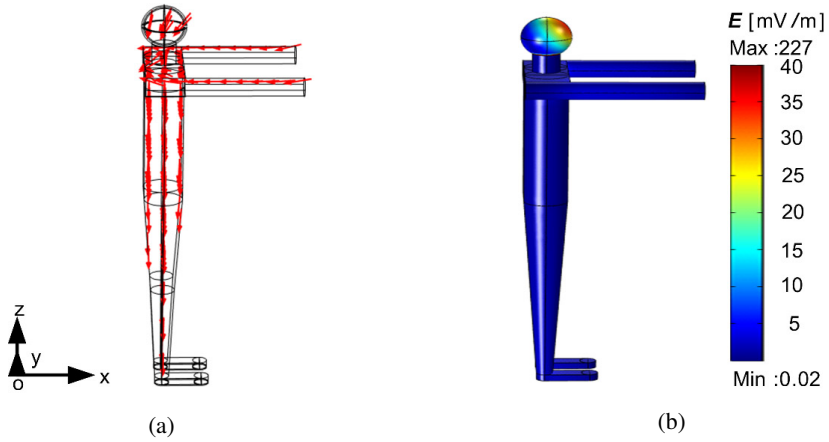

(a) (b)

Fig. 6. Electric field strength in the body of high signal operator: (a) arrow plot; (b) *E*-field distribution

analyze the distribution of the induced electric field in the head tissue, we analyze the electric field of three head layers, namely the scalp, skull, and brain. The *E*-field distribution in such layers of the operator's head is shown in Fig. 7.

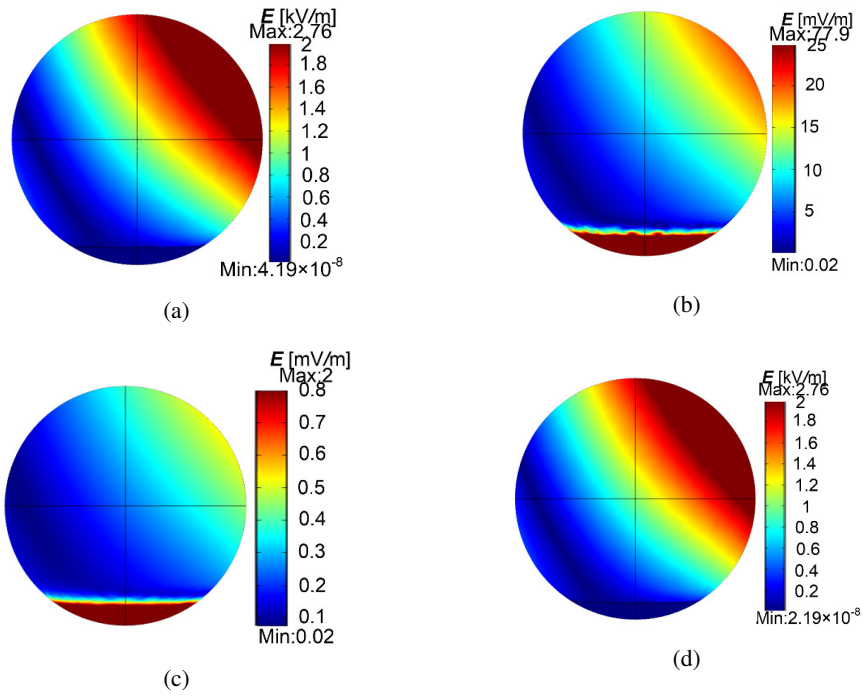

(a) (b) (c) (d)

Fig. 7. Distribution of electric field strength in head layers: (a) scalp; (b) skull; (c) brain; (d) head

Fig. 7 shows that the electric field values in the scalp, skull, brain, and head layers are, respectively, as follows: 4.19×10^{-8} kV/m – 2.76 kV/m, 0.02 mV/m – 7.9 mV/m, 0.02 mV/m – 2 mV/m, and 2.19×10^{-8} kV/m – 2.76 kV/m. The maximum electric field intensity in the head layer is 2.76 kV/m, and it is mainly distributed at the boundary between the scalp and the air near the contact wire and neck side. The maximum electric field strength in the scalp layer is 3.54×10^4 times that on the skull surface and 1.38×10^8 times that in the brain layer. These results indicate that the electric field is mainly distributed in the scalp tissue and attenuates rapidly, thus effectively protecting the inner head layers of the skull and brain. In the case of high voltage, the lower part of the skull and brain is easier to gather charges, so the E-field induced by the charges is relatively large.

To further analyze the distribution of the induced electric field in the head tissue, we selected mid cross-sections for further studies. The mid cross-sections of the high-signal operator's head are, respectively, as follows: $x = -2.63$ m, the $y0z$ slice; $y = 0$ m, the $x0z$ slice and $z = 5.408$ m, the $x0y$ slice. The electric field distribution inside the head is shown in Fig. 8.

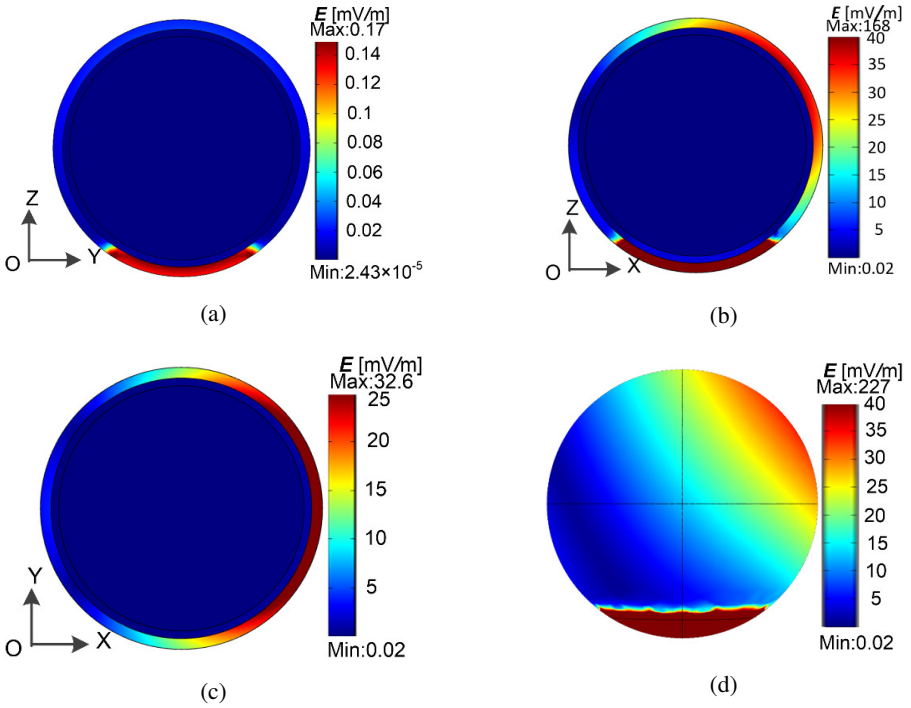

Fig. 8. Electric field distribution in different planes of the operator's head: (a) $x = -2.63$ m; (b) $y = 0$ m; (c) $z = 5.408$ m; (d) head

Fig. 8 shows that the maximum electric field strength inside the human head is 227 mV/m, which equals to the maximum value of the electric field within a human body. The electric field distribution at $x = -2.63$ m, the $y0z$ slice for head is 2.43×10^{-5} mV/m – 0.17 mV/m, at

y = 0 m, the $x0z$ slice for head is 0.02 mV/m – 168 mV/m, at z = 5.408 m, the $x0y$ slice for brain is 0.02 mV/m – 32.6 mV/m, at the internal part of head is 0.02 mV/m – 227 mV/m. The electric field is mainly distributed in the scalp near side of the contact wire and the neck side of the head.

Figs. 7 and 8 show that the electric field intensity decay rapidly at the boundary between the layers and inside of the high signal operator's head. To observe the changing attenuation of the electric field intensity in space, on the head surface, and inside the head, a head model was cut by a 300 mm straight line passing through the head center (–2630, 0, 5408 mm) along the negative direction of the x-axis (Fig. 9). The distribution of the electric field strength along this path is shown in Fig. 10.

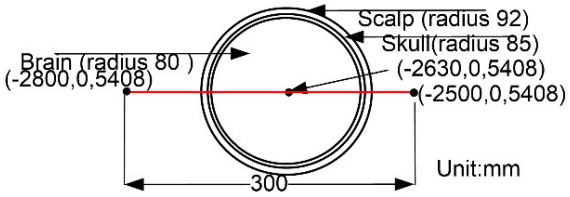

Fig. 9. Dimmensions of head layers and the cutting line

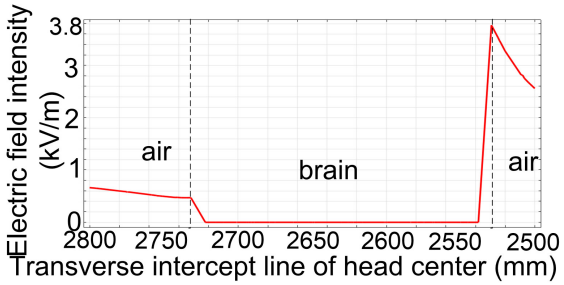

Fig. 10. Distribution of electric field strength along the given path for the singal-track railway

As shown in Fig. 10, the electric field strength increases sharply at the scalp near the contact wire side and at the interface of the space but decreases sharply inside the head. The electric field strength increases slowly at the far side of the scalp and outer boundary of the computational domain.

4.2. Analysis for double-track railway

The distance between two contact wires is 5.5 m for a double-track railway, as presented in Fig. 3. The simulation calculation is performed after loading the source of contact wire 1 and contact wire 2 with a frequency of 50 Hz and a voltage of 27.5 kV. The electric field distribution inside the operator's body, different head layers and different planes of the head are similar to the single-track railway. But the values are different. The peak values of the electric field strength at different parts of the body are shown in Table 3.

Table 3 illustrates the peak values of the electric field strength at different parts of the body for double-track railways higher than that of the single-track railways.

Table 3. The peak values of the electric field strength at different parts of body for double-track railway

Different part of body	**Electric field strength (mV/m)**	**Higher than that for the single-track railway**
Inside the operator's body	310	83
Layer of scalp	3.42×10^6	6.6×10^5
Layer of skull	107	29.1
Layer of brain	2.75	0.75
Head surface	3.42×10^6	6.6×10^5
$x = -2.63$ m, $y0z$ slice	232	231.83
$y = 0$ m, $y0z$ slice	231	63
$z = 5.408$ m, $x0y$ slice	39.5	6.9
Inside the operator's head	310	83

To observe the changing attenuation of the electric field strength in space, on the head surface, and inside the head, a head model was cut by a 300 mm straight line passing through the head center (–2630, 0, 5408) mm along the negative direction of the x-axis (see Fig. 9). The distribution of the electric field strength along this path is shown in Fig. 11.

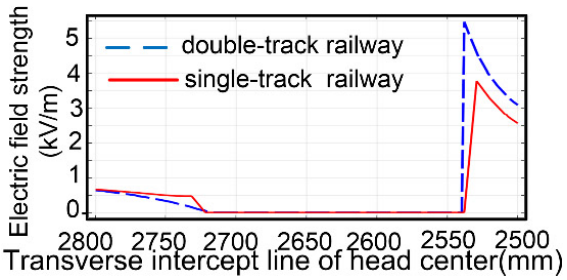

Fig. 11. Distribution of electric field strength along the given path for the single- and double-track railways

Fig. 11 shows that the maximum electric field on the head surface near the double-track railway is bigger than that near the single-track railway. The electric field strength decreases rapidly at the scalp near the contact wire side for the two analyzed cases.

5. Comparison of electric field strengths with ICNIRP's occupational exposure limits for the high signal operator

According to the occupational exposure limits for a power frequency of 50 Hz given in the ICNIRP standard [10], the electric field limits are divided into reference levels for spatial averaged external electric fields and basic restrictions for internal electric fields. The basic restrictions of

the electric field inside the human body are divided into the central nervous system (CNS) of the head (corresponding to the analyzed brain layer) and the whole body. The specific numerical comparison is shown in Table 4.

Table 4. Comparison of maximum E-field strengths with ICNIRP's occupational exposure limits

Working conditions	**Space electric field (kV/m)**	**Internal electric field (mV/m)**	
	Head surface	**Brain layer**	**Whole body**
Single-track railway	2.76	0.14	227
Double-track railway	3.42	0.19	310
ICNIRP's occupational exposure limits [10]	10 (reference level)	100 (basic restriction)	800 (basic restriction)

As shown in Table 4, the ICNIRP's occupational exposure reference level for the space-averaged electric field is equal to 10 kV/m. The maximum E-values in the head layers of the high signal operator are 27.6% and 34.2% of the reference level when the operator works in a single-track railway and a double-track railway, respectively. These values are all under the ICNIRP's the reference level. The maximum electric fields of the brain layer (head's CNS) and the whole body are 0.19% and 38.75% of the occupational exposure basic restrictions, respectively. The comparison with the ICNIRP's occupational exposure limits shows that the electric field intensities of the head surface, the internal body, and brain layer of a high signal operator under an electromagnetic exposure are within specified limits.

For a frequency of 50 Hz, the limit of electric field strength is divided into the low action levels (ALs) for external electric fields and the exposure limit values (ELVs) for internal electric fields in EU Directive [11]. The sensory ELVs (corresponding to the analyzed brain layer) and the specific numerical comparison are shown in Table 5.

Table 5. Comparison of maximum E-field strengths with EU Directive's exposure limit values

Working conditions	**Workplace electric field (kV/m)**	**Internal electric field (mV/m)**
Single-track railway	1.78	0.14
Double-track railway	1.95	0.19
EU Directive [11]	10 (low ALs)	140 (sensory effects ELVs)

As shown in Table 5, the EU Directive's low action levels (low ALs) for a workplace electric field is equal to 10 kV/m. The maximum E-values in the head layers of the high signal operator are 17.8% and 19.5% of the low ALs when the operator works in a single-track railway and a double-track railway, respectively. The maximum electric fields of the brain layer are 0.1% and 0.135% of the EU Directive's ELVs, respectively. The comparison with the EU Directive's ALs and sensory effect ELVs show that the electric field strength of the workplace electric field, and internal electric field of a high signal operator under an electromagnetic expoure are within specified limits.

6. Conclusion

A finite element simulation engine is used herein to calculate the electric field intensity of a high signal operator working on single- and double-track railways. The following conclusions are obtained through the performed numerical analysis.

1. The electric field distribution around the contact wires changes depending on whether a high signal operator works on a single- or double-track railway. The distortion occurs at the boundary of the head and the air. The maximum E-value in the head layer is 2.76 kV/m, which is four orders higher than that inside the head (227 mV/m) during high signal operation in a single-track railway.
2. During high signal exposure on a double-track railway, the maximum electric field strength on the worker's head surface is 3.42 kV/m, which is 34.2% of the ICNIRP's occupational exposure reference level and 34.2% of the EU Directive's low ALs. The maximum electric field intensities inside the human body and brain are 310 mV/m and 0.19 mV/m, respectively. These values are significantly lower than the ICNIRP's occupational exposure basic restrictions.
3. The maximum electric field intensities in the central nerve system (brain layer) of a high signal operator's head in single- and double-track railway settings are 0.14% and 0.19% of the occupational exposure basic restrictions, respectively. These values are 0.10% and 0.135% of the EU Directive's sensory ELVs, respectively.
4. The electric field strength in the whole body of a high signal operator caused by the contact wires in a double-track railway is greater than that in a single-track railway. These values are lower than the ICNIRP's occupational exposure limits.

In summary, the work of a high signal operator in the vicinity of single-track and double-track railways poses no risk of exposing him to harmful levels of electric fields.

Acknowledgements

The authors would like to acknowledge the financial support by the National Natural Science Foundation of China (Grant Nos. 51567015, 51867014), by the Department of Education of Gansu Province under Grant 2018D-08, by the Youth fund of Lanzhou Jiaotong University 2017040, and by the Opening Foundation of Key Laboratory of Opto-Electronic Technology and Intelligent Control of Ministry of Education, Lanzhou Jiaotong University KFKT2020-15. We are grateful to the peer reviewers who provided us with valuable comments during reviewing the manuscript.

References

[1] Wyszkowska J.W., Jankowska M., Gas P., *Electromagnetic fields and neurodegenerative diseases*, Przeglad Elektrotechniczny, vol. 95, no. 1, pp. 129–133 (2019).

[2] Mahaki H., Jabarivasal N., Sardarian K., Zamani A., *Effects of various densities of 50 Hz electromagnetic field on serum IL-9, IL-10, and TNF-α levels*, The International Journal of Occupational and Environmental Medicine, vol. 11, no. 1, pp. 24–32 (2020).

[3] Wertheimer N., Leeper E.D., *Electrical wiring configurations and childhood cancer*, American Journal of Epidemiology, vol. 109, no. 3, pp. 273–284 (1979).

[4] Di G., Dong L., Xie Z., Xu Y., Xiang J., *Effects of power frequency electric field exposure on kidney*, Ecotoxicology and Environmental Safety, vol. 194, no. 110354, pp. 1–6 (2020).

[5] Syrek P., Skowron M., *The impact of overhead lines for employees with stents*, IOP Conference Series: Materials Science and Engineering, vol. 200, no. 012013, pp. 1–6 (2017).

[6] Gas P., Miaskowski A., *Implant Safety Tool Application to Assist the Assessment of Radio-Frequency Radiation Exposure*, Journal of Ecological Engineering, vol. 20, no. 10, pp. 24–33 (2019).

[7] Oancea C.D., Calin F., Golea V., *On the Electromagnetic Field in the Surrounding Area of Railway Equipment and Installations*, 2019 International Conference on Electromechanical and Energy Systems (SIELMEN), Craiova, Romania, pp.1–5 (2019).

[8] Wen Y.H., Hou W.X., *Research on Electromagnetic Compatibility of Chinese High Speed Railway System*, Chinese Journal of Electronics, vol. 29, no. 1, pp. 16–21 (2020).

[9] Wrobel Z., *The Electromagnetic Compatibility in Researches of Railway Traffic Control Devices*, Lecture Notes in Electrical Engineering, vol. 452, pp. 275–287 (2018).

[10] ICNIRP, *Guidelines for limiting exposure to time-varying electric and magnetic fields (1 Hz to 100 kHz)*, Health Physics, vol. 99, no. 6, pp. 818–836 (2010).

[11] 2013/35/EU: *Directive of the European Parliament and of the Council of 26 June 2013 on the minimum health and safety requirements regarding the exposure of workers to the risks arising from physical agents (electromagnetic fields)*, Official Journal of the European Union, L 179, pp. 1–21 (2013).

[12] https://timgsa.baidu.com/timg?image&quality=80&size=b9999_10000&sec=1606369465878&di=311321a9c108936454933bf4a777536f&imgtype=0&src=http%3A%2F%2Fy.zdmimg.com%2F201711%2F08%2F5a02beb474f797348.jpg_e600.jpg, accessed on December 2020.

[13] http://5b0988e595225.cdn.sohucs.com/images/20181002/5b1720a89c7a456c9cebb2696008ae14.jpeg, accessed on December 2020.

[14] Gas P., Wyszkowska J., *Influence of multi-tine electrode configuration in realistic hepatic RF ablative heating*, Archives of Electrical Engineering, vol. 68, no. 3, pp. 521–533 (2019).

[15] Stuchly M.A., Dawson T.W., *Human body exposure to power lines: relation of induced quantities to external magnetic fields*, Health Physics, vol. 83, no. 3, pp. 333–340 (2002).

[16] Lu M., Ueno S., *Computational study toward deep transcranial magnetic stimulation using coaxial circular coils*, IEEE Transactions on Biomedical Engineering, vol. 62, no. 12, pp. 2911–2919 (2015).

[17] Bidi M., *Biological risk assessment of high-voltage transmission lines on worker's health of electric society*, Archives of Electrical Engineering, vol. 69, no. 1, pp. 57–68 (2020).

[18] Bakker J.F., Paulides M.M., Neufeld E., Christ A., Chen X.L., Kuster N., Van Rhoon G.C., *Children and adults exposed to low-frequency magnetic fields at the ICNIRP reference levels: Theoretical assessment of the induced electric fields*, Physics Medicine Biology, vol. 57, no. 7, pp. 1815–1829 (2012).

[19] Tian R., Lu M., *Safety assessment of electromagnetic exposure in high-speed train carriage with full passengers*, Annals of Work Exposures and Health, vol. 64, no. 8, pp. 838–851 (2020).

[20] Alvin R.T., *Ergonomics diagram – human factors in design*, translated by Zhu T., China Architecture and Building Press (1998).

[21] Rush S., Driscoll D.A., *Current distribution in the brain from surface electrodes*, Anaesthesia and Analgesia, vol. 47, no. 6, pp. 717–723 (1968).

[22] http://niremf.ifac.cnr.it/tissprop/htmlclie/htmlclie.php, accessed on December 2020.

[23] Keikko T., Isokorpi J., Korpinen L., *Practical problems in calculating electric fields of transmission lines*, Eleventh International Symposium on High Voltage Engineering, London, UK, vol. 2, pp. 103–106 (1999).